Synthesis, Crystal Structure, and Potentiometry of Pyridine-Containing Tetraaza Macrocyclic Ligands with Acetate Pendant Arms

Won D. Kim,[†] Duane C. Hrncir,[†] Garry E. Kiefer,[‡] and A. Dean Sherry*,[†]

Department of Chemistry, University of Texas at Dallas, Richardson, Texas 75083-0688, and Designed Chemicals R & D, Dow Chemical Co., Freeport, Texas 77541

Received July 19, 1994[⊗]

Tetraazamacrocycles containing the pyridine moiety as part of the cyclic backbone and acetate pendant arms were prepared. The resulting products were characterized by high resolution NMR (^{1}H and ^{13}C) spectroscopy and single-crystal X-ray diffraction. Single-crystal X-ray diffraction data were obtained for the following compounds: py[12]aneN$_4$·HCl, $C_{11}H_{19}N_4Cl$, orthorhombic Pnma (No. 62), a = 10.304(6) Å, b = 9.160(2) Å, c = 13.552(2) Å, Z = 4, Mo Kα, λ = 0.710 69, R = 0.037, R_w = 0.036; and BP2A·2HCl·3H$_2$O, $C_{18}H_{22}N_4O_4Cl_2$·3H$_2$O, triclinic $P\bar{1}$ (No. 2), a = 10.201(0) Å, b = 13.267(3) Å, c = 8.612(6) Å, α = 97.676(2)°, β = 105.821(0)°, λ = 86.363(7)°, Z = 2, Mo Kα, λ = 0.710 69, R = 0.039, R_w = 0.038. In addition, protonation constants (log K_{HnL}) and metal ion stability constants (log K_{ML}) for BP2A (log $K_{H_{1-4}L}$ = 9.57, 5.99, 2.59, 2.22; log K_{MgL} = 8.9; log K_{CaL} = 10.0; log K_{GdL} = 14.5) and PC2A (log $K_{H_{1-5}L}$ = 12.5, 5.75, 3,28, 2.38, ~1; log K_{MgL} = 8.4, log K_{CaL} = 10.0, log K_{GdL} = 16.6) were determined using potentiometric and NMR pH titrations. These values agree well with previously reported literature values for analogous ligand systems.

Introduction

In recent years the interest in polyazamacrocyclic paramagnetic and radioactive metal ion chelates has grown considerably, largely due to biomedical applications such as (1) magnetic resonance imaging (MRI) contrast agents,[1] (2) NMR shift and relaxation probes of the dynamic solution conformation of molecules, (3) shift reagents for NMR-active cations,[2] and (4) diagnostic and therapeutic radiopharmaceuticals.[3] Consequently, investigation of macrocyclic complexes by electrochemical, spectral, structural, kinetic, and thermodynamic evaluations has received considerable attention. As a result of these studies, a number of paramagnetic metal chelates are now used clinically as bioconjugates for monoclonal antibody radioisotope labeling and as MRI contrast agents.

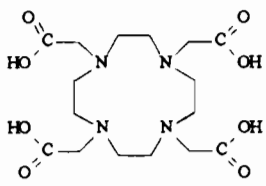

DOTA

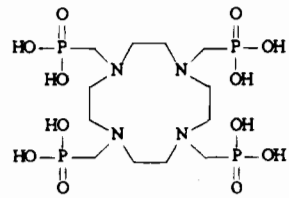

DOTP

The ligand, DOTA, derived from tetraazacyclododecane (CYCLEN) forms one of the most thermodynamically stable and kinetically inert complexes with the trivalent lanthanide cations of any known chelate.[4] These properties make Gd(DOTA)$^-$ one of the most effective and safest MRI contrast enhancement[5] agents available. The complex formed between lanthanide metals and the methylenephosphonate analog, DOTP, has also been examined in some detail[6] and the Tm^{3+} complex, $Tm(DOTP)^{5-}$, is proving to be a versatile $^{23}Na^+$ shift agent, both for perfused tissues and for *in vivo* animal studies.

All current commercially available MRI contrast agents are classified as general extracellular agents. These nonspecific "perfusion agents" distribute throughout the extracellular spaces in the body before being excreted through the kidneys. The value of perfusion agents is well documented, particularly for highly vascularized brain lesions which typically exhibit enhanced contrast following infusion of the chelate. However, the perfusion agents' lack of tissue specificity requires dose levels to be kept relatively high in order to obtain observable contrast enhancement. Alternatively, a much lower dose level could be employed if the contrast agent were delivered to a specific organ or region of the body, resulting in a high localized concentration. Although much more involved from a synthetic point of view, this approach promises greater sensitivity at reduced dose levels with the added potential for diagnosing organ function and metabolism. Furthermore, such tissue-specific agents may be valuable nuclear therapeutic agents when complexed with appropriate radioactive isotopes.

The concept of using organ/tissue specific metal chelates for MRI originates from the development of radiopharmaceutical agents for various applications. Organ/tissue specific radiopharmaceuticals are presently employed for diagnostic evaluations of hepatobiliary and kidney function, brain imaging, myocardial imaging,[7] and bone imaging. Many of these tissue specific agents are ^{99m}Tc based complexes with their tissue specificity resulting from the suitable combination of lipophilicity, molecular weight, and ionic charge in the ligands.[8]

One might envision several possible methods for tissue-specfic delivery of a MRI contrast agent. The agent could be

* To whom correspondence should be addressed.
† University of Texas at Dallas.
‡ Dow Chemical Co.
⊗ Abstract published in *Advance ACS Abstracts,* March 15, 1995.

(1) Sherry, A. D. *J. Less-Common Metals* **1989**, *149*, 133.
(2) Sherry, A. D.; Geraldes, C. F. G. C. In *Lanthanide Probes in Life, Chemical and Earth Sciences, Theory and Practice*; Bunzli J. C. G., Choppin, G. R., Eds.; Elsevier: Amsterdam, 1989; Chapter 4.
(3) Jurisson, S.; Berning, D.; Jia, W.; Ma, D. *Chem. Rev.* **1993**, *93*, 1137.
(4) (a) Cacheris, W. P.; Nickle, S. J.; Sherry, A. D. *Inorg. Chem.* **1987**, *26*, 958. (b) Brucher, E.; Laurenczy, G.; Makra, Z. *Inorg. Chim. Acta* **1987**, *139*, 141. (c) Wang, X; Jin, T.; Comblin V.; Lopez-Mut, A.; Merciny, E.; Desreux, J. F. *Inorg. Chem.* **1992**, *31*, 1095.
(5) Runge, V. M. *Enhanced Magnetic Resonance Imaging*; C. V. Mosby Co.: St. Louis, MO, 1989.
(6) (a) Lázár, I.; Hrncir, D. C.; Kim, W. D.; Kiefer, G. E.; Sherry, A. D. *Inorg. Chem.* **1992**, *31*, 4422. (b) Geraldes, C. F. G. C.; Sherry, A. D.; Kiefer, G. E. *J. Magn. Reson.* **1992**, *97*, 290. (c) Sherry, A. D.; Geraldes, C. F. G. C.; Cacheris, W. P. *Inorg. Chim. Acta* **1987**, *139*, 137. (d) Sherry, A. D.; Malloy, C. R.; Jefferey, F. M. H.; Cacheris, W. P.; Geraldes, C. F. G. C. *J. Magn. Reson.* **1988**, *76*, 528.

0020-1669/95/1334-2225$09.00/0

designed so that lipophilic character, molecular weight, and/or ionic charge of the chelate is readily varied. A more elaborate approach would involve the incorporation of functionality known to be recognized by receptor sites at a specific organ.

In this report, we focus on variations in chelate ionic charge using ligands which generate positively charged complexes upon complexation of a trivalent lanthanide. Our approach was to modify the basic 12-membered macrocycle structure by incorporating one or two pyridine moieties.

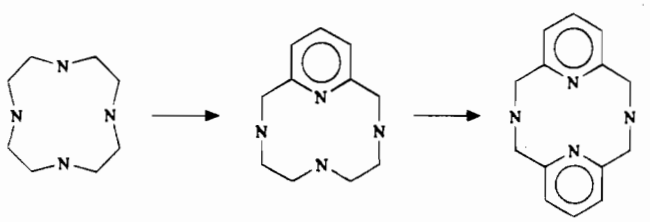

The effects of this change are obvious reduction of secondary amine sites for pendant or ligating group attachment and increased rigidity of the macrocyclic ring. One consequence of this reduction in total ligating group functionality is a lowering of the anionic or negative charge in the resulting M·L complexes. We speculated that the added rigidity of the macrocycle would also influence complexation kinetics and thermodynamic properties. Also, since pyridyl nitrogens have substantially lower pK_a's than tertiary nitrogens, the overall basicity of these ligands should be reduced, and hence proton competition with the bound metal in at neutral pH would be reduced.

As a part of our continuing effort, we herein report the synthesis and complexation properties of the pyridine-based tertraazamacrocycles.

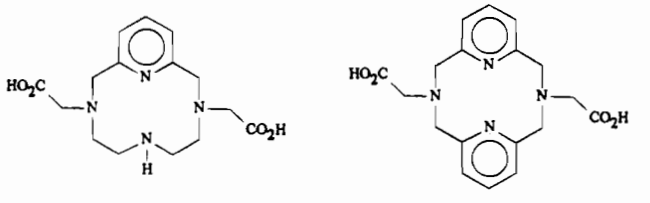

PC2A **BP2A**

This report includes the synthesis of PC2A and BP2A, single-crystal X-ray studies for py[12]aneN$_4$·HCl, and BP2A·2HCl·3H$_2$O, and determination of protonation constants (log K_{HL}) and metal stability constants (log K_{ML}) of the ligands by potentiometric titrations. A report including relaxometry, luminescence measurement, electrophoresis, and animal biodistribution studies of lanthanide(III) complexes of these ligands is reported in a companion paper.

Experimental Section

Synthesis of Ligands. General Materials and Methods. All reagents were obtained from commercial suppliers and used as received without further purification. NMR spectra were recorded on JEOL FX200, Bruker AC-250, or GE GN-500 spectrometers at 298 K unless otherwise indicated. ^{1}H spectra in D_2O were recorded by employing a solvent suppression pulse sequence ("PRESAT",[9] homonuclear presaturation). ^{1}H spectra are referenced to residual chloroform (in $CDCl_3$) at δ 7.26 or external dioxane (in D_2O) at δ 3.55. ^{13}C spectra reported are proton decoupled. Assignments of $^{13}C\{^1H\}$ chemical shifts were aided by DEPT[10] (distortionless enhancement by polarization transfer) experiments. $^{13}C\{^1H\}$ spectra are referenced to the center peak of $CDCl_3$ at δ 77.00 (in $CDCl_3$) or external dioxane at δ 66.66 (in D_2O). Semipreparative ion-exchange chromatographic separations were performed at low pressure (<60 psi) using either a Dionex 2010i or DX-300 system fitted with hand-packed Q-Sepharose (anion exchange) or SP-Sepharose (cation exchange) glass column (Omni-Fit), and with on-line UV detector at 268 nm for eluent monitoring.

3,6,9,15-Tetraazabicyclo[9.3.1]pentadeca-1(15),11,13-triene,[11] py[12]-aneN$_4$, (**1**), 2,11-diaza[3.3](2,6)pyridinophane,[12] py$_2$[12]aneN$_4$, (**2**), *N*,*N*′-bis(*p*-tosyl)ethylenediamine disodium salt,[13] (**3**), and 2,6-bis(chloromethyl)pyridine,[14] (**4**), were prepared using literature methods. Crystals of py[12]aneN$_4$·HCl suitable for single-crystal X-ray crystallography were obtained from slow evaporation of concentrated aqueous solution whose pH was previously adjusted to ~10.

3,9-Bis(sodium methylenesulfonato)-3,6,9,15-tetraazabicyclo-[9.3.1]pentadeca-1(15),11,13-triene (5). An aqueous solution (10.0 mL) of **1** (1.03 g, 5.0 mmol) was added with concentrated HCl (0.5 mL) and stirred for 10 min to ensure complete dissolution. The resulting solution had a pH of 8.6. $HOCH_2SO_3Na$ (1.37 g, 10.2 mmol) was then added along with 5 mL of DI water, and the solution heated at 60 °C for 10 min resulting in a pH drop to 5.6. After cooling, the pH was adjusted to 9.0 with 1 M NaOH followed by freeze-drying to give the desired product as a white solid (quantitative): ^{1}H NMR (D_2O) δ 2.87 (t, $-CH_2-$, 5,7-cyclic, J_{H-H} = 5.2 Hz, 4 H), 3.18 (t, $-CH_2-$, 4,8-cyclic, J_{H-H} = 5.2 Hz, 4 H), 3.85 (s, $-CH_2-$, 2,10-cyclic, 4 H), 4.11 (s, N$-CH_2-$S, 4 H), 7.03 (d, 3,5-py, J_{H-H} = 7.7 Hz, 2 H), 7.55 (t, 4-py, J_{H-H} = 7.7 Hz, 1 H); $^{13}C\{^1H\}$ NMR (D_2O) δ 48.52 ($-CH_2-$, 5,7-cyclic), 54.04 ($-CH_2-$, 4,8-cyclic), 58.92 ($-CH_2-$, 2,10-cyclic), 75.09 (N$-CH_2-$S), 123.90 (3,5-py), 141.37 (4-py), 161.89 (2,6-py).

3,9-Bis(methylenenitrile)-3,6,9,15-tetraazabicyclo[9.3.1]pentadeca-1(15),11,13-triene (6). NaCN (0.6 g, 12.24 mmol) was added to an aqueous solution (10.0 mL) of **5** (2.26 g, 5 mmol) and the reaction mixture stirred for 3 h at room temperature. The pH of the resulting reaction mixture was approximately 10. Upon pH adjustment to >13 (with concentrated NaOH), the product precipitated and was extracted with $CHCl_3$ (3 × 20 mL), dried over anhydrous $MgSO_4$, and filtered. Upon removal of solvent *in vacuo*, the desired product was isolated as a waxy white powder (1.00 g, 71%): ^{1}H NMR ($CDCl_3$) δ 2.03 (s, br, $-CH_2-$, 5,7-cyclic, 4 H), 2.64 (m, $-CH_2-$, 4,8-cyclic, 4 H), 3.82 (s, N$-CH_2-$CN, 4 H), 3.90 (s, $-CH_2-$, 2,10-cyclic, 4 H), 7.14 (d, 3,5-py, J_{H-H} = 7.6 Hz, 2 H), 7.62 (t, 4-py, J_{H-H} = 7.6 Hz, 1 H); $^{13}C\{^1H\}$ NMR ($CDCl_3$) δ 46.08 ($-CH_2-$, 5,7-cyclic), 46.64 (N$-CH_2-$CN), 52.89 ($-CH_2-$, 4,8-cyclic), 60.78 ($-CH_2-$, 2,10-cyclic), 115.31 ($-CN$), 122.02 (3,5-py), 137.57 (4-py), 157.33 (2,6-py).

3,6,9,15-Tetraazabicyclo[9.3.1]pentadeca-1(15),11,13-triene-3,9-diacetic acid PC2A (7). An HCl solution (37%, 30 mL) of **6** (2.5 mmol) was heated at reflux for 2 h. After cooling, the aqueous solution was evaporated to dryness followed by coevaporation with fresh DI water (2 × 10 mL) to eliminate excess HCl. The pH of the solution was adjusted to 7 with concentrated NaOH (50%) and the resulting neutral solution chromatographed on cation exchange column (SP-Sepharose, 1.5 × 50 cm) eluting first with DI water then with 1 M HCl. The acidic fraction containing product was evaporated to dryness followed by coevaporation with fresh DI water (3 × 10 mL) to eliminate excess HCl. The final product was isolated as a white solid upon freeze drying of the concentrated aqueous solution (quantitative yield): ^{1}H NMR (D_2O) δ 2.84 (s, br, $-CH_2-$, 5,7-cyclic, 4 H), 3.18 (m, $-CH_2-$,

(7) (a) Leppo, J. A.; DePuey, E. G.; Johnson, Lynne, *J. Nucl. Med.* **1991**, *32*, 2012. (b) Holman, B. L.; Jones, A. G.; Lister-James, J.; et al. *J. Nucl. Med.* **1984**, *25*, 1350. (c) Narra, R. K.; Nunn, A. D.; Kuczynski, B. L.; Feld, T.; Wedeking, P.; Eckelman, W. C. *J. Nucl. Med.* **1989**, *30*, 1830.

(8) (a) Treher, E. N.; Francesconi, L. C.; Gougoutas, J. Z.; Malley, M. F.; Nunn, A. D. *Inorg. Chem.* **1989**, *28*, 3411. (b) Linder, K. E.; Malley, M. F.; Gougoutas, J. Z.; Unger, S. E.; Nunn, A. D. *Inorg. Chem.* **1990**, *29*, 2428.

(9) ASPECT-3000 NMR Software Manual. Bruker, Part # Z30319, Feb. 1987, p 99.

(10) (a) Morris, G. A. In *Topics in ^{13}C NMR Spectroscopy*; Levy, G. C., Ed., Wiley New York, 1984; pp 179–196. (b) Bendall, M. R.; Doddrell, D. M.; Pegg, D. T.; Hull, W. E. DEPT. Bruker Analytische Messtechnik, Karlsruhe, Germany, 1982.

(11) Stetter, H.; Frank, W.; Mertens, R. *Tetrahedron* **1981**, *37*, 767.

(12) Bottino, F.; Grazia, M. D.; Finocchiaro, P.; Fronczek, F. R.; Mamo, A.; Pappalardo, S. *J. Org. Chem.* **1988**, *53*, 3521.

(13) Koyama, H.; Yoshino, T. *Bull. Chem. Soc. Jpn.* **1972**, *45*, 481.

(14) Baker, W.; Buggle, K. M.; McOmie, J. F. W.; Watkins, D. A. M. *J. Chem. Soc.* **1958**, 3594.

4,8-cyclic, 4 H), 3.77 (s, N−CH_2-−CO_2H, 4 H), 4.35 (s, −CH_2−, 2,-10-cyclic, 4 H), 7.63 (d, 3,5-py, J_{H-H} = 7.9 Hz, 2 H), 8.23 (t, 4-py, J_{H-H} = 7.9 Hz, 1 H); $^{13}C\{^1H\}$ NMR (D_2O) δ 47.45 (−CH_2−, 5,7-cyclic), 54.33 (−CH_2−, 4,8-cyclic), 59.73 (N−CH_2−CO_2H), 60.36 (-CH_2-, 2,10-cyclic), 127.20 (3,5-py), 149.31 (4-py), 155.60 (2,6-py), 177.74 (C=O).

2,11-Diaza[3.3](2,6)pyridinophane-*N,N'*-diacetic acid-BP2A (8). Bromoacetic acid (275 mg, 1.98 mmol, excess) was added to a stirred aqueous solution (1 mL) of **2** (82.4 mg, 0.58 mmol) and the pH of the reaction mixture maintained above 10 by adding small portions of concentrated NaOH (50%) until no more caustic was needed to keep the pH > 11 (~30 min). The reaction mixture was then heated (60 °C) for 2 h, then cooled to room temperature and the pH of the reaction mixture adjusted to 7. The solution was then chromatographed on cation exchange column (SP-Sepharose, 1.5 × 50 cm) eluting first with DI water then with 1 M HCl. The acidic fraction containing product was evaporated to dryness followed by coevaporation with fresh DI water (3 × 2 mL) to eliminate excess HCl. The final product was isolated as a white solid upon freeze drying of the concentrated aqueous solution from above (quantitative yield): ^1H NMR (D_2O) δ 4.17 (s, N−CH_2−C, 4 H), 4.43 (s, −CH_2−, cyclic, 8 H), 7.15 (d, 3,5-py, J_{H-H} = 7.9 Hz, 4 H), 7.66 (t, 4-py, J_{H-H} = 7.9 Hz, 2 H); $^{13}C\{^1H\}$ NMR (D_2O) δ 61.44 (N−CH_2−C), 61.70 (−CH_2−, cyclic), 127.46 (3,5-py), 146.84 (4-py), 154.37 (2,6-py), 175.62 (C=O). Crystals of BP2A·2HCl·3H_2O suitable for single-crystal X-ray crystallography were obtained from slow cooling of a hot concentrated aqueous solution.

Crystal Structure Determinations. X-ray intensity data for py[12]aneN$_4$·HCl, and BP2A·2HCl·3H_2O were collected on an Enraf-Nonius CAD4 diffractometer using Mo Kα radiation (λ = 0.70930 Å) and the ω-2θ scan technique.

py[12]aneN$_4$·HCl. A single crystal of py[12]aneN$_4$·HCl suitable for X-ray analysis was mounted in a thin-walled glass capillary in a random orientation. Cell constants and an orientation matrix for data collection were obtained from least-squares refinement, using the setting angles of 25 centered reflections measured by the computer-controlled diagonal slit method of centering. The data were collected at a temperature of 23 ± 1°. The scan rate varied from 2 to 20°/min in ω. Data were collected to a maximum 2θ of 50.0°. The scan range was determined as a function of θ to correct for the separation of the Kα doublet; the scan width was calculated as follows: θ scan width = 0.8 + 0.340 tan θ. Moving-crystal moving-counter background counts were made by scanning an additional 25% above and below this range. Thus the ratio of peak counting time to background counting time was 2:1. The counter aperture was also adjusted as a function of θ. The horizontal aperture width ranged from 4.0 to 4.2 mm; the vertical aperture was set at 4.0 mm. The diameter of the incident beam collimator was 0.7 mm and the crystal to detector distance was 21 cm. For intense reflections an attenuator was automatically inserted in front of the detector; the attenuator factor was 12.9. From the systematic absences ($hk0$ $h = 2n$, $0kl$ $k + l = 2n$) and subsequent least-squares refinement, the space group was determined to be *Pnma* (No. 62). A total of 1202 reflections were collected to a maximum 2θ of 50.0°. As a check on crystal and electronic stability 3 representative reflections were measured every 60 min. There was a total gain in intensity of 0.5%. A linear decay correction was applied. The correction factors on I ranged from 0.997 to 1.000 with an average value of 0.999. Lorentz and polarization corrections were applied to the data. The linear absorption coefficient is 2.8 cm^{-1} for Mo Kα radiation. No absorption correction was made and no extinction correction was necessary. The structure was solved by direct methods. Hydrogen atoms were were included (located from the difference Fourier electron density maps) in the refinement. The structure was refined by full-matrix-least squares methods where the function minimized was $\sum w(|F_o| - |F_c|)^2$ where the weight, w, is defined as 1.0 for all observed reflections. Scattering factors were taken from Cromer and Waber.[15] Anomalous dispersion effects were included in F_c;[16] the values for $\Delta f'$ and $\Delta f''$ were those of Cromer.[17] Only the 862 reflections having intensities greater than 3.0 times their standard deviation were used in the refinements. The final cycle of refinement included 108 variable parameters and converged with unweighted and weighted agreement factors of $R = \sum||F_o| - |F_c||/\sum|F_o| = 0.037$ and $R_w = [\sum w(|F_o| - |F_c|)^2/\sum w|F_o|^2]^{1/2} = 0.036$. The standard deviation of an observation of unit weight was 0.77. Pertinent crystallographic data are given in Table 1. All calculations were performed on a MicroVAX II computer using the SDP/VAX set of programs.

Table 1. Summary of the Crystallographic Data for py[12]aneN$_4$·HCl and BP2A·2HCl·3H_2O

	py[12]aneN$_4$·HCl	BP2A·2HCl·3H_2O
formula	$C_{11}H_{19}N_4$·Cl	$C_{18}H_{22}N_4O_4$·2Cl·H_2O
fw	242.75	483.35
space group	*Pnma* (No. 62) orthorhombic	$P\bar{1}$ (No. 2) triclinic
cell const		
a, Å	10.304(6)	10.201(0)
b, Å	9.160(2)	13.267(3)
c, Å	13.552(2)	8.612(6)
α, deg		97.676(2)
β, deg		105.821(0)
λ, deg		86.363(7)
V, Å^3	1279.2	1111.0
Z	4	2
D_{calc}, g/cm^3	1.260	1.445
radiation	Mo Kα	Mo Kα
max cryst. dimens, mm	0.2 × 0.5 × 0.8	0.4 × 0.4 × 0.7
scan width, deg	0.8 + 0.34 tan θ	0.8 + 0.34 tan θ
std reflcns	2, −1, 5; 3, 0, 5; 4, 1, 3	1, 4, 0; 2, 2, −2; 0, 1, 3
% decay of stds	0.5	0.5
no. of reflcns measd	1202	3902
data collcn range (2θ), deg	4 < 2θ < 50	4 < 2θ < 50
no. of obsd reflcns	862	2722
no. of params varied	108	310
R^a	0.037	0.039
$R_w{}^b$	0.036	0.038

$^a R = \sum||F_o| - |F_c||/\sum|F_o|$. $^b R_w = [\sum w(|F_o| - |F_c|)^2/\sum w|F_o|^2]^{1/2}$.

BP2A·2HCl·3H_2O. This structure was determined as described above. Hydrogen atoms bonded to carbon atoms were included (calculated) in the refinement but restrained to ride on the carbon atom to which they are bonded. Hydrogen atoms bonded to nitrogen and oxygen atoms were located from the difference Fourier electron density maps. Pertinent crystallographic data are given in Table 1.

Determination of Protonation and Stability Constants. Equipment and Materials. Potentiometric titrations were performed using a Dosimat 665 auto buret (Brinkmann) along with an 8103 Ross combination pH electrode (Orion) interfaced to an Accumet 925 pH meter (Fisher). The pH electrode was checked with standard pH 4.00, 7.00, and 10.00 buffers (Fisher, 0.05 M) for efficiency. Then the final calibration parameters (effective slope and zero potential, E^0, were determined by titrating a solution of known hydrogen ion concentration in 0.1 M KCl. p[H^+], that is −log[H^+], values during experimental titration runs were then calculated from millivolt readings directly from the pH meter and converted to p[H^+] using the calibration parameters. pK_w was determined from data obtained in the alkaline range of the titration and found to be 13.80. The DI water was ultrapure bioresearch grade (< 18 MΩ/cm) which was filtered (0.45 μm nylon filter) and freshly degassed prior to used. KOH solutions (~0.1 M) were prepared by dissolving ultrapure KOH (99.99%, semiconductor grade, Aldrich) into freshly degassed DI water followed by standardization by potentiometric titration[18] against KHP (potassium hydrogen phthalate, Fisher). The CO_2 content was determined from a Gran's plot.[19] Solutions of $MgCl_2$, $CaCl_2$, and $GdCl_3$ were standardized complexometrically (EDTA/Eriochrome Black T for $MgCl_2$ and $CaCl_2$, and Xylenol Orange for $GdCl_3$ as indicators). Ligand concentrations were determined potentiometrically from the plots of Δ pH/Δ mL (KOH) vs mL (KOH).

Potentiometric Determination of Protonation Constants. The following describes a typical experiment. A titration sample (5.000 mL, ~4 mM) was prepared by adding 0.200 mL of the ligand stock solution (~0.1 M) to 4.800 mL of 0.1 M KCl solution to keep the ionic

(15) Cromer, D. T.; Waber, J. T. *International Tables for X-ray Crystallography*; The Kynoch Press: Birmingham, England, 1974; Vol. IV, Table 2.2B.
(16) Iber, J. A.; Hamilton, W. C. *Acta Crystallogr.* **1964**, *17*, 781.
(17) Cromer, D. T. *International Tables for X-ray Crystallography*; The Kynoch Press: Birmingham, England, 1974; Vol. IV, Table 2.3.1
(18) Gran, G. *Analyst* **1952**, *77*, 661.
(19) Rossotti, F. J. C; Rossotti, H. *J. Chem. Educ.* **1965**, *42*, 375.

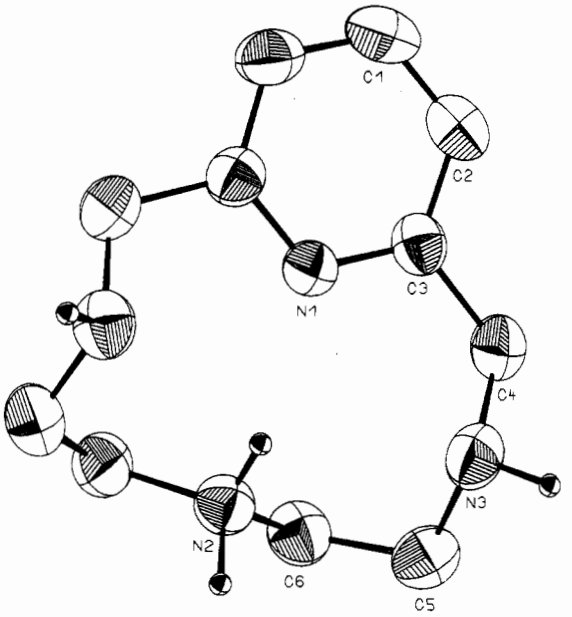

Figure 1. ORTEP plot (50% probability thermal ellipsoids) of the structure of py[12]aneN$_4$·HCl with the numbering scheme. Hydrogen atoms, except those bonded to nitrogens, have been omitted for clarity.

strength of the solution constant (0.1 M). A layer of cyclohexane and blanket of slightly positive pressure of N_2 atmosphere were maintained to protect the solution from CO_2 and the cell was thermostated at 25 °C. After sample equilibration (30 min), it was titrated with standard KOH (0.1 M) with increments of 0.002 mL (with a 3−10 s delay) while the titration data (pH vs mL base) were captured into a disk file. Multiple (n = 3) sets of data files containing 170−190 points were used in calculation of the protonation constants. The protonation constants were calculated using the program PKAS.[20]

NMR Titration of PC2A. A solution of PC2A was made up in D_2O and the pD was adjusted with DCl or CO_2-free KOD. The NMR titrations[21] were carried out using CO_2-free KOD and were corrected for a deuterium isotope effect (pD = pH + 0.40).[22] The ^{1}H spectra were recorded as a function of added KOD. These spectra were recorded on a single solution below pH ~ 12, where the KOD concentration was varied and the solution pD measured. Above this pH, individual solutions were prepared from a PC2A stock solution at pH 12 by adding known amounts of KOD. −log[H$^+$] was calculated for each solution by assuming that the ligand does not contribute to the proton concentration at these high pH values. All high resolution spectra were recorded on a General Electric GN-500 Spectrometer in 5 mm tubes at 25 °C using a GE variable temperature accessory. Probe temperatures were accurate to ±0.5 °C.

Potentiometric Determination of Metal Ion Stability Constants. In a typical experiment, a titration sample (5.000 mL, ~4 mM) was prepared by adding 0.200 mL of the ligand stock solution (~0.1 M) to an equivalent amount of the metal stock solution (~0.1 M). KCl solution (0.1 M) was then added to keep the ionic strength of the sample solution constant. A layer of cyclohexane and blanket of slightly positive pressure of N_2 atmosphere were maintained to exclude CO_2 from the sample solution, and the cell was thermostated at 25 °C. After equilibration (30 min), each sample was titrated with standard KOH (0.1 M) with increments of 0.002 mL while the titration data (pH vs mL base) were captured into a disk file. The delay between each KOH addition (3 to 90 s) was adjusted to ensure that complete equilibrium was reached before each addition of the titrant. Multiple (n = 3) sets of data files containing 170−190 points were used in calculation of the metal ion stability constants. The metal ion stability constants were calculated using the program BEST[23] considering 1:1 complex formation.

(20) Motekaitis, R. J.; Martell, A. E. *Can. J. Chem.* **1982**, *60*, 168.
(21) Macomber, R. S. *J. Chem. Educ.* **1992**, *69*, 375.
(22) Delgado, R.; Fraústo da Silva, J. J. R.; Amorim, M. T. S.; Cabral, M. F.; Chaves, S.; Costa, J. *Anal. Chim. Acta.* **1991**, *245*, 271.

Table 2. Positional Parameters and Their Estimated Standard Deviations for py[12]aneN$_4$·HCl

atom	x	y	z	B,[a] Å^2
Cl	1.05072(9)	0.250	0.68364(7)	3.43(2)
N(1)	0.6471(3)	0.250	0.3944(2)	3.45(6)
N(2)	0.7977(3)	0.250	0.5655(2)	3.62(7)
N(3)	0.7854(2)	−0.0009(3)	0.4431(2)	4.12(5)
C(1)	0.4688(4)	0.250	0.2431(3)	5.0(1)
C(2)	0.5142(3)	0.1197(3)	0.2808(2)	4.41(7)
C(3)	0.6043(3)	0.1239(3)	0.3570(2)	3.59(5)
C(4)	0.6558(3)	−0.0164(3)	0.4011(2)	4.40(6)
C(5)	0.7932(3)	−0.0169(3)	0.5505(2)	4.73(7)
C(6)	0.7362(3)	0.1143(3)	0.6024(2)	4.20(6)

[a] Anisotropically refined atoms are given in the form of the isotropic equivalent displacement parameter defined as (4/3)[$a^2B(1,1) + b^2B(2,2) + c^2B(3,3) + ab(\cos\gamma)B(1,2) + ac(\cos\beta)B(1,3) + bc(\cos\alpha)B(2,3)$].

Table 3. Bond Angles (deg) and Distances (Å) for py[12]aneN$_4$·HCl[a]

	Bond Angles		
C(4)−N(3)−C(5)	115.4(2)	C(2)−C(3)−C(4)	120.3(3)
C(1)−C(2)−C(3)	118.5(3)	N(3)−C(4)−C(3)	113.2(2)
N(1)−C(3)−C(2)	121.8(3)	N(3)−C(5)−C(6)	111.2(2)
N(1)−C(3)−C(4)	117.9(2)	N(2)−C(6)−C(5)	110.1(2)
	Bond Distances		
N(1)−C(3)	1.336(3)	C(1)−C(2)	1.380(4)
N(2)−C(6)	1.482(3)	C(2)−C(4)	1.389(4)
N(3)−C(4)	1.459(4)	C(3)−C(4)	1.514(4)
N(3)−C(5)	1.465(4)	C(5)−C(6)	1.512(4)

[a] Numbers in parentheses are estimated standard deviations in the least significant digits.

Results and Discussion

Synthesis of Ligands. The preparation of py[12]aneN$_4$ and py$_2$[12]aneN$_4$ were achieved according published methods.[11,12] BP2A was prepared by reacting py$_2$[12]aneN$_4$ with bromoacetic acid at high pH in aqueous media. PC2A was prepared by adjusting (with HCl) an aqueous solution of py[12]aneN$_4$ to pH 8.6 (this acidification also helped dissolution of py[12]aneN$_4$) and adding a stoichiometric amount of the formaldehyde−sodium bisulfite addition compound. Unlike numerous other methods we have tried in the past which generated complex mixtures of multiple species requiring chromatographic separation, this method generates only the intended product (3,9-disubstituted) in essentially quantitative yield. This product was then converted to PC2A via substitution with NaCN followed by acid hydrolysis. The cyano derivative also serves as a convenient intermediate for additional modification at the N-6 position.

Crystal Structure of py[12]aneN$_4$ and BP2A. The structure of py[12]aneN$_4$ is shown in Figure 1 (ORTEP drawing of py[12]aneN$_4$·HCl). Table 1 lists the pertinent crystallographic data. The fractional atomic coordinates, and bond angles and distances for non-hydrogen atoms are given in Tables 2 and 3, respectively. Four molecules of py[12]aneN$_4$ constitute a centrosymmetric orthorhombic unit cell where each molecule is composed of two asymmetric units through a mirror plane. The bond distances and angles are very typical for this type of organic molecule. An important feature of this structure is, however, the location of the first protonation site for this molecule (py[12]aneN$_4$) at the N-6 [N(2) in Figure 1] position. This was determined by locating the hydrogen in the difference Fourier electron density maps. This is consistent with protonation scheme of py[12]aneN$_4$ reported[24] where the protonation scheme was determined by ^{1}H-NMR titrations. The location of a single

(23) Motekaitis, R. J.; Martell, A. E. *Can. J. Chem.* **1982**, *60*, 2403.

Table 4. Positional Parameters and Their Estimated Standard Deviations for BP2A·2HCl·3H$_2$O

atom	x	y	z	B,[a] Å^2
CL(1)	0.70427(8)	0.11518(7)	0.4225(1)	3.95(2)
CL(2)	1.07492(8)	0.37760(6)	0.68742(9)	3.47(2)
O(1)	0.6312(2)	0.3991(2)	0.9450(3)	5.76(7)
O(2)	0.5747(2)	0.4081(2)	0.6818(3)	5.46(6)
O(3)	1.5489(2)	0.1217(2)	0.8079(3)	4.38(6)
O(4)	1.4517(2)	0.1425(2)	0.5481(3)	4.75(6)
O(100)	0.9998(2)	0.1465(2)	0.6584(2)	3.50(5)
O(101)	0.8067(3)	0.3343(2)	0.3879(3)	5.10(6)
O(102)	0.6126(3)	0.4719(2)	0.2553(3)	6.15(7)
N(1)	1.1663(2)	0.3356(2)	1.0502(3)	2.50(5)
N(2)	0.8831(2)	0.2966(2)	0.9311(3)	2.37(5)
N(3)	1.2946(2)	0.1810(2)	0.8837(3)	2.80(5)
N(4)	1.0708(2)	0.1312(2)	0.9904(3)	2.57(5)
C(1)	1.2681(3)	0.3674(3)	1.3747(4)	3.77(8)
C(2)	1.1325(3)	0.3878(2)	1.3061(3)	3.13(6)
C(3)	1.0802(3)	0.3696(2)	1.1415(3)	2.45(6)
C(4)	0.9319(3)	0.3820(2)	1.0541(4)	3.09(7)
C(5)	0.8479(3)	0.2082(2)	0.9942(4)	3.44(7)
C(6)	0.9749(3)	0.1490(2)	1.0728(3)	2.63(6)
C(7)	1.0000(3)	0.1158(2)	1.2226(4)	3.25(7)
C(8)	1.1237(3)	0.0689(2)	1.2868(4)	3.62(7)
C(9)	1.2226(3)	0.0576(2)	1.2035(4)	3.46(7)
C(10)	1.1949(3)	0.0902(2)	1.0527(4)	2.84(6)
C(11)	1.2967(3)	0.0861(2)	0.9533(4)	3.70(7)
C(12)	1.3734(3)	0.2621(3)	0.9926(4)	4.02(8)
C(13)	1.2981(3)	0.3109(2)	1.1129(4)	2.91(6)
C(14)	1.3516(3)	0.3272(3)	1.2782(4)	3.57(7)
C(15)	0.7820(3)	0.3258(2)	0.7883(3)	3.23(7)
C(16)	0.6549(3)	0.3811(2)	0.8163(4)	3.15(7)
C(17)	1.3107(3)	0.1687(3)	0.7202(4)	3.69(7)

[a] Anisotropically refined atoms are given in the form of the isotropic equivalent displacement parameter defined as $(4/3)[a^2B(1,1) + b^2B(2,2) + c^2B(3,3) + ab(\cos\gamma)B(1,2) + ac(\cos\beta)B(1,3) + bc(\cos\alpha)B(2,3)]$.

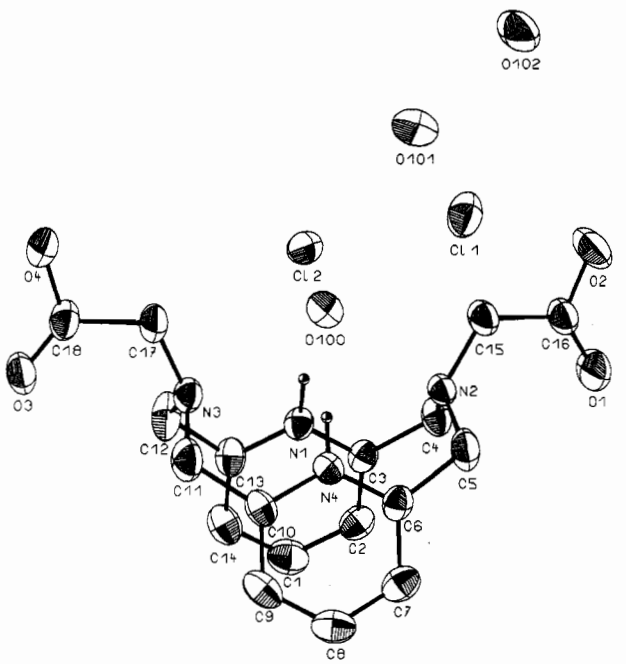

Figure 2. ORTEP plot (50% probability thermal ellipsoids) of the structure of BP2A·2HCl·3H$_2$O. Hydrogen atoms, except those bonded to nitrogens, have been omitted for clarity.

proton on N-6 indicated that this was the most basic nitrogen in the macrocycle. The protonation constants[24] of N-3 and N-9 are considerably lower suggesting that sulfomethylation[25] may enable selective alkylation of N-3 and N-9 similar to that found for DO2A[26] (the 1,7-diacetate of CYCLEN). This finding was the basis for the novel regioselective 3,9-alkylation of py[12]-aneN$_4$.

Table 5. Bond Angles (deg) and Distances (Å) for BP2A·2HCl·3H$_2$O[a]

Bond Angles			
C(3)−N(1)−C(13)	123.6(2)	C(7)−C(8)−C(9)	120.5(3)
C(4)−N(2)−C(5)	114.5(2)	C(8)−C(9)−C(10)	119.4(3)
C(4)−N(2)−C(15)	113.5(2)	N(4)−C(10−C(9)	118.5(3)
C(5)−N(2)−C(15)	114.3(2)	N(4)−C(10)−C(11)	117.3(3)
C(11)−N(3)−C(12)	115.1(2)	C(9)−C(10)−C(11)	124.2(3)
C(11)−N(3)−C(17)	114.9(2)	N(3)−C(11)−C(10)	111.5(2)
C(12)−N(3)−C(17)	114.5(3)	N(3)−C(12)−C(13)	110.6(3)
C(6)−N(4)−C(10)	123.5(2)	N(1)−C(13)−C(12)	115.8(2)
C(2)−C(1)−C(14)	120.3(3)	N(1)−C(13−C(14)	118.7(3)
C(1)−C(2)−C(3)	119.9(3)	C(12)−C(13)−C(14)	125.4(3)
N(1)−C(3)−C(2)	118.2(3)	C(1)−C(14)−C(13)	119.1(3)
N(1)−C(3)−C(4)	117.3(3)	N(2)−C(15)−C(16)	116.7(2)
C(2)−C(3)−C(4)	124.5(3)	O(1)−C(16)−O(2)	123.9(3)
N(2)−C(4)−C(3)	112.5(2)	O(1)−C(16)−C(15)	124.5(3)
N(2)−C(5)−C(6)	110.7(2)	O(2)−C(16)−C(15)	111.5(3)
N(4)−C(6)−C(5)	116.9(3)	N(3)−C(17)−C(18)	116.9(2)
N(4)−C(6)−C(7)	118.6(2)	O(3)−C(18)−O(4)	125.6(3)
C(5)−C(6)−C(7)	124.5(3)	O(3)−C(18)−C(17)	125.6(3)
C(6)−C(7)−C(8)	119.2(3)	O(4)−C(18)−C(17)	108.9(2)
Bond Distances			
O(1)−C(16)	1.188(4)	C(1)−C(2)	1.373(4)
O(2)−C(16)	1.303(4)	C(1)−C(14)	1.382(5)
O(3)−C(18)	1.187(3)	C(2)−C(3)	1.366(4)
O(4)−C(18)	1.323(4)	C(3)−C(4)	1.504(4)
N(1)−C(3)	1.351(4)	C(5)−C(6)	1.512(4)
N(1)−C(13)	1.343(3)	C(6)−C(7)	1.373(4)
N(2)−C(4)	1.456(3)	C(7)−C(8)	1.377(4)
N(2)−C(5)	1.460(4)	C(8)−C(9)	1.379(5)
N(2)−C(15)	1.452(3)	C(9−C(10)	1.374(4)
N(3)−C(11)	1.462(4)	C(10)−C(11)	1.510(5)
N(3)−C(12	1.453(4)	C(12)−C(13)	1.508(5)
N(3−C(17)	1.449(4)	C(13)−C(14)	1.372(4)
N(4)−C(6)	1.349(4)	C(15)−C(16)	1.510(4)
N(4)−C(10)	1.344(3)	C(17)−C(18)	1.516(4)

[a] Numbers in parentheses are estimated standard deviations in the least significant digits.

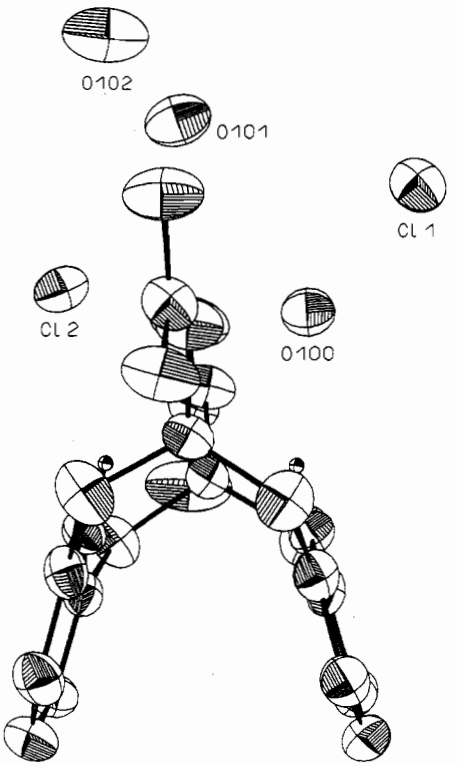

Figure 3. "Side view", ORTEP plot (50% probability thermal ellipsoids), of the structure of BP2A·2HCl·3H$_2$O. Hydrogen atoms, except those bonded to nitrogens, have been omitted for clarity.

The structure of BP2A is shown in Figure 2 (ORTEP drawing of BP2A·2HCl·3H$_2$O) and Figure 3 (ORTEP drawing, "side

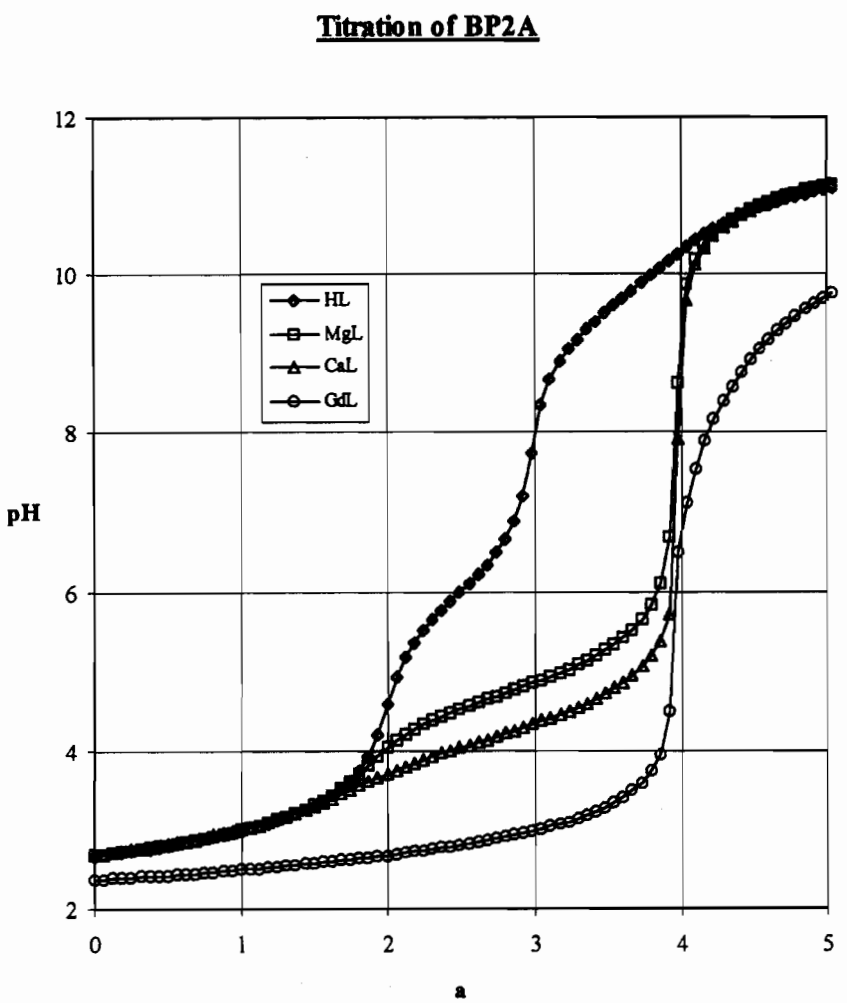

Figure 4. Potentiometric titration curves of BP2A with and without metal (Mg^{2+}, Ca^{2+}, and Gd^{3+}) present. "**a**" is the equivalents of OH^- per ligand equivalent.

view"). Table 1 lists the pertinent crystallographic data. The fractional atomic coordinates, and bond angles and distances for all non-hydrogen atoms are given in Tables 4 and 5, respectively. Two asymmetric units constitute a triclinic unit cell where an asymmetric unit consists of a diprotonated organic cation (+2 charged), two Cl^- anions, and three water molecules. The four nitrogens are on the same side of the macrocyclic ring, resulting in a conformation common to tetraoxo- and tetraaza-cyclododecanes.[27] The overall geometry of the ring is similar to that reported for similar macrocycles (DOTA·Gd·Na·$5H_2O$[28] and DOTP[6a]) resulting in a conformation common for this type of molecule. However, the macrocyclic ring appears to be more rigid due to the aromatic pyridine rings. Figure 3 shows a side view of the two pyridine rings. The angle produced by the two pyridine rings is very sharp and the distance between the two rings is indeed very close. Examination of the C−O bond lengths reveals that both carboxylates are protonated (carboxylic acid). Additionally, judging by the bond distances, O(1)−C(16) [1.188(4) Å] and O(3)−C(18) [1.187(3) Å] are double bonds (carbonyl group), while O(2)−C(16) [1.303(4) Å] and O(4)−C(18) [1.323(4) Å] are single bonds (hydroxyl group). Since both carboxylates were protonated, the two Cl^- counteranions indicated that two ring nitrogens must be protonated. These protons were located, from difference Fourier electron density maps, on the two pyridine nitrogens [N(1) and N(4) in Figure 2] rather than on the tertiary nitrogens [N(2) and N(3)], even though tertiary amines are considered more basic than pyridine [e.g., $pK_a(R_3N) \sim 9-11$, pK_a(pyridine) = 5.2[29]]. Thus, although the value of log K_1 in BP2A suggests that the first protonation occurs at a tertiary nitrogen (see below), the most stable structure of BP2A after four protons have been added (two nitrogens and two caboxylates), involve protonation of both pyridine nitrogens.

Protonation and Metal Ion Stability Constants. The protonation constants and metal ion stability constants for BP2A and PC2A were determined by potentiometric titrations while the highest protonation constant (log K_1) of PC2A was determined by ^{1}H-NMR titration. Potentiometric titration curves (with and without metal present) of H_2BP2A·2HCl with KOH is shown in Figure 4. These data indicate that two protons are titrated below pH ~ 4.5, one between pH 4.5 and 8, and one between pH 8 and 10.5. Potentiometric titration curves (with

(24) Costa, J.; Delgado, R. *Inorg. Chem.* **1993**, *32*, 5257.
(25) van Westrenen, J.; Sherry, A. D. *Bioconjugate Chem.* **1992**, *3*, 524.
(26) Torres, D. A. Synthesis and Characterization of New Ligands from 1,4,7,10-tetraazacyclododecane: Prospects for Use as MRI Contrast Agents. Thesis, The University of Texas at Dallas, Dallas, TX, 1992.
(27) (a) Risen, A.; Zehnder, M.; Kaden, T. A. *Helv. Chim. Acta* **1986**, *69*, 2067. (b) Sacurai, T.; Kobayashi, K.; Tsuboyama, K.; Tsuboyama, S. *Acta. Crystallogr.* **1978**, *B34*, 1144. (c) Riesen A.; Zehnder, M.; Kaden, T. A. *J. Chem. Soc., Chem. Commun.* **1985**, 1336.
(28) (a) Dubost, J. P.; Leger, J. M.; Langlois, M. H.; Meyer, D.; Schaefer, M. *C. R. Acad. Sci. Paris, Ser. 2* **1991**, *312*, 349. (b) Reibenspies, J. H.; Anderson, O. P. *Abstracts of Papers*; 193rd National Meeting of the American Chemical Society, Denver, CO, American Chemical Society: Washington, DC, 1987; INOR 165.
(29) Loudon, G. M. *Organic Chemistry*; Addison-Wesley Publishing Company, Inc.: Reading, Massachusetts, 1984; pp 1187 (Table 26.4) and 1266.

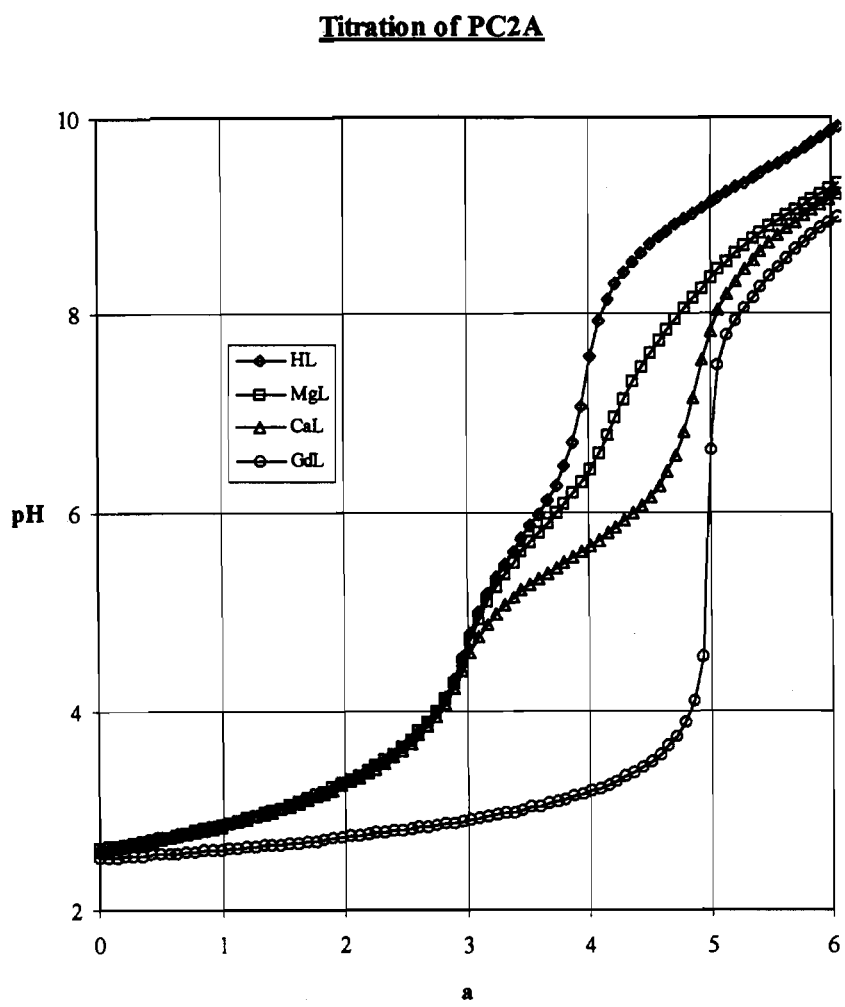

Figure 5. Potentiometric titration curves of PC2A with and without metal (Mg^{2+}, Ca^{2+}, and Gd^{3+}) present. "a" is the equivalents of OH^- per ligand equivalent.

and without metal present) of $H_2PC2A{\cdot}3HCl$ with KOH is shown in Figure 5. The data indicate that three protons are titrated below pH ~ 4.5, one between pH 4.5 and 7.5, and a fifth at much higher pH. The highest protonation constant of PC2A was determined by a NMR titration. The titration curves shown in Figure 6 were consistent with the highest protonation occurring at the secondary amine (N6) trans to the pyridine. The protonation constants determined by the standard computational method using these data are listed in Table 6 along with previously reported values for the other structurally similar ligands.

The stability constants (log K_{ML}) of Mg^{2+}, Ca^{2+}, and Gd^{3+} with BP2A and PC2A complexes were determined by direct potentiometric titration (the titration curves are shown in Figures 4 and 5, respectively). Each of these ions form 1:1 complexes quite rapidly (including the trivalent lanthanide, Gd^{3+}), and in the process all protons are released from the ligand. No evidence for formation of MH_xL species for any of the metal ion complexes was found. The metal ion stability constants determined for BP2A and PC2A are listed in Table 7 along with previously reported values for other structurally related ligands.

The protonation constants of the compounds, determined in the present work, show trends similar to those of other polyazamacrocyclic compounds. The highest protonation constant of PC2A (log K_1 = 12.5) corresponds to protonation of the secondary nitrogen atom opposite the pyridine ring, while the second protonation constant (log K_2 = 5.75) likely represents protonation of the pyridine nitrogen. However, while the second protonation constant (log K_2 = 5.99) of BP2A is in expected range for protonation of a pyridine nitrogen, the first protonation constant (log K_1 = 9.57) is much lower than in the case of PC2A. The reason for this may be related to the flexibility and the size of cavity within these macrocycles. While PC2A has some flexible regions as part of its macrocyclic ring, BP2A does not have such flexibility. This can be easily be seen from the "side view" (Figure 3) of BP2A. The only flexible parts of the molecule are two tertiary nitrogens (N-2 and N-3), and these nitrogens simply act as hinges connecting the two pyridine rings. In contrast, the nitrogen trans to the pyridine nitrogen in PC2A should be quite flexible. The protonation constant of this nitrogen may be unusually high because, upon protonation, this nitrogen can align with the pyridine nitrogen to form a strong intra-ring hydrogen bond. In BP2A, the two tertiary nitrogens have very little flexibility and, indeed, protonation at these sites probably would not be stabilized by intra-ring hydrogen bonds. Thus, the highest protonation constant is only 9.57. It is also interesting to compare these values with the first and the second protonation constants of DO2A. The highest two protonation constants of (log K_1 = 10.91 and log K_2 = 9.45) DO2A are typical of protonation at two secondary nitrogens opposite each other in a macrocyclic ring.

It has been reported that the CYCLEN derivatives (i.e., DOTA, DOTP, and DO2A etc.) form complexes too slowly with the trivalent lanthanide (Gd^{3+}) for normal potentiometric titrations, thus the values reported were from "batch or out-of-cell methods." However, the formation (complexation) kinetics of BP2A and PC2A with Gd^{3+} are fast enough for potentiometric titration, and hence, the metal ion stability constants reported in this study were directly determined from the potentiometric

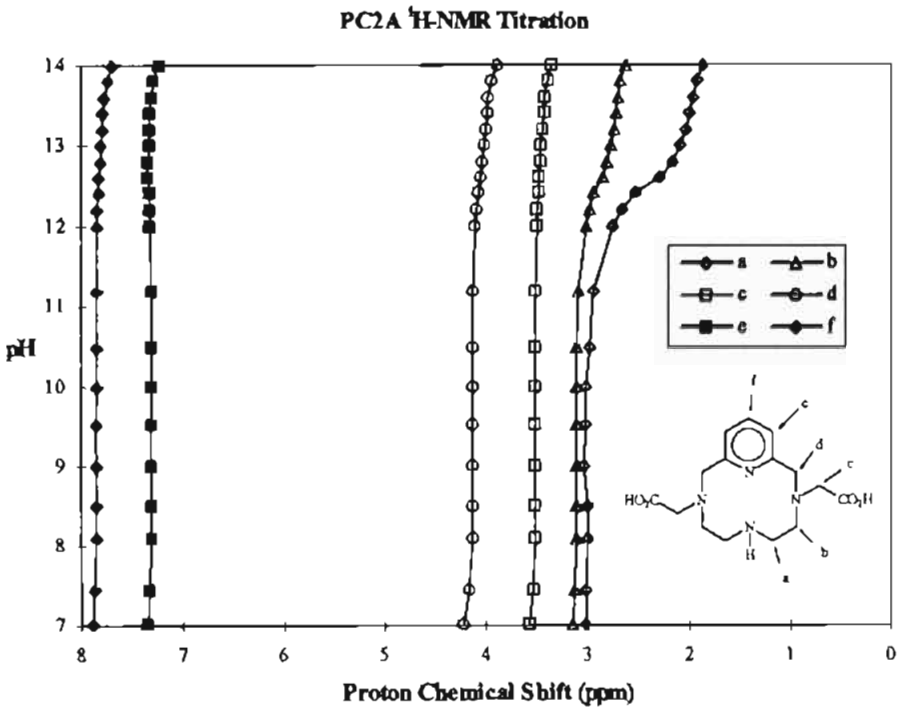

Figure 6. ^{1}H chemical shifts of the nonexchangeable protons of PC2A recorded as a function of solution pH. Chemical shift assignments are shown in the figure. The curve corresponding to the macrocyclic ethylene protons next to the N-6 position (a) was used to calculate the highest protonation constant of PC2A.

Table 6. Comparison of Protonation Constants

	log K_1	log K_2	log K_3	log K_4
BP2A	9.57	5.99	2.59	2.22
	0.01	0.03	0.01	0.01
PC2A	12.5[a]	5.75	3.28	2.38
	0.1	0.01	0.01	0.01
DO2A[b]	10.91	9.45	4.09	3.18
DOTA[c]	11.22	9.75	4.37	4.36
py[12]aneN4[d]	10.33	7.83	1.27	< 1
CYCLEN[e]	10.70	9.70	1.73	0.94

[a] From NMR titration. [b] Torres, D. A. Synthesis and Characterization of New Ligands from 1,4,7,10-Tetraazacyclododecane: Prospects for Use as MRI Contrast Agent. Thesis, The University of Texas at Dallas, 1992. [c] (a) Delgado, R.; Frausto da Silva, J. J. R. *Talanta* **1982**, *29*, 815. (b) Delgado, R.; Frausto da Silva, J. J. R.; Vaz, M. C. T. A. *Inorg. Chim. Acta* **1984**, *90*, 185. [d] Costa, J.; Delgado, R. *Inorg. Chem.* **1993**, *32*, 5257. [e] Kodama, M.; Kimura, E. *J. Chem. Soc., Dalton Trans.* **1980**, 327.

Table 7. Comparison of Metal Ion Stability Constants (log K_{ML})

	Mg^{2+}	Ca^{2+}	Gd^{3+}
BP2A	8.9	10.0	14.5
	0.1	0.1	0.1
PC2A	8.4	10.0	16.6
	0.1	0.1	0.1
DO2A[a]	10.87	15.37	19.42
DOTA	11.03[b]	15.85[b]	24.6[c]
CYCLEN[d]	2.25	3.12	

[a] Torres, D. A. Synthesis and Characterization of New Ligands from 1,4,7,10-Tetraazacyclododecane: Prospects for Use as MRI Contrast Agent. Thesis, The University of Texas at Dallas, 1992. [b] (a) Delgado, R.; Frausto da Silva, J. J. R. *Talanta* **1982**, *29*, 815. (b) Delgado, R.; Frausto da Silva, J. J. R.; Vaz, M. C. T. A. *Inorg. Chim. Acta* **1984**, *90*, 185. [c] Cacheris, W. P.; Nickle, S. K.; Sherry, A. D. *Inorg. Chem.* **1987**, *26*, 958. [d] Ruangpornvisuti, V. W.; Probst, M. M.; Rode, B. M. *Inorg. Chim. Acta* **1988**, *144*, 22.

titration curves using the standard computer best fitting calculations. The aromatic pyridine ring substructure(s) present in these molecules are likely responsible for these rapid kinetics. This observation is consistent with our findings from the crystallographic structure determinations that these macrocyclic ring appear to have considerably less conformational flexibility than CYCLEN derivatives. In the case of BP2A (Figure 3), one can easily see that the ligand is highly "preorganized" for metal coordination.

Upon comparison of the metal ion stability constants for the ligands BP2A, PC2A and DO2A, several interesting trends emerge. First, the Gd^{3+} stability constants fall in the order expected; as secondary nitrogen donors are replaced by less basic pyridine nitrogen donors, the complexes become less stable, DO2A > PC2A > BP2A. However, this trend does not hold with Ca^{2+} and Mg^{2+}. The stability of Ca(BP2A) and Ca(PC2A) were equal while Mg(BP2A) was actually more stable than Mg(PC2A). We attribute this to the smaller size of the highly preorganized BP2A macrocyclic cavity, which should favor complexation of the smaller Mg^{2+} ion. In this case, this factor apparently outweighs the decreased basicity considerations.

Acknowledgment. This work was supported by grants from the Robert A. Welch Foundation (AT-584) and Dow Chemical Co. (for portions of the research performed at UTD).

Supplementary Material Available: Tables of crystal data, atomic positional parameters, bond distances and angles, and anisotropic thermal parameters of all atoms for py[12]aneN$_4$·HCl and BP2A·2HCl·3H$_2$O (14 pages). Ordering information is given on any current masthead page.

IC9408462